AD NUMBER

AD469693

LIMITATION CHANGES

TO:

Approved for public release; distribution is unlimited.

FROM:

**Distribution authorized to U.S. Gov't. agencies and their contractors;
Administrative/Operational Use; AUG 1965. Other requests shall be referred to Ballistic Systems Division, Attn: BSQT, Norton AFB, CA 92409.**

AUTHORITY

OCRD D/A memo, 1 Apr 1968

AVCO EVERETT

RESEARCH LABORATORY

a division of
AVCO CORPORATION

MEASUREMENTS OF THE RADIATION FROM AN ABLATION CONTAMINATED BOUNDARY LAYER UNDER SIMULATED FLIGHT CONDITIONS

K. L. Wray, P. H. Rose and H. E. Koritz

RESEARCH REPORT 226
August 1965

supported jointly by
BALLISTIC SYSTEMS DIVISION
DEPUTY FOR BALLISTIC MISSILE RE-ENTRY SYSTEMS
AIR FORCE SYSTEMS COMMAND
Norton Air Force Base, California
under Contract No. AF 04(694)-414

ADVANCED RESEARCH PROJECTS AGENCY
monitored by the
ARMY MISSILE COMMAND
UNITED STATES ARMY
Redstone Arsenal, Alabama
under Contract No. DA-19-020-AMC-0210
(part of Project DEFENDER)

This research is a part of Project DEFENDER, sponsored by the Advanced Research Projects Agency, Department of Defense, under ARPA Order No. 525.

DISCLAIMER NOTICE

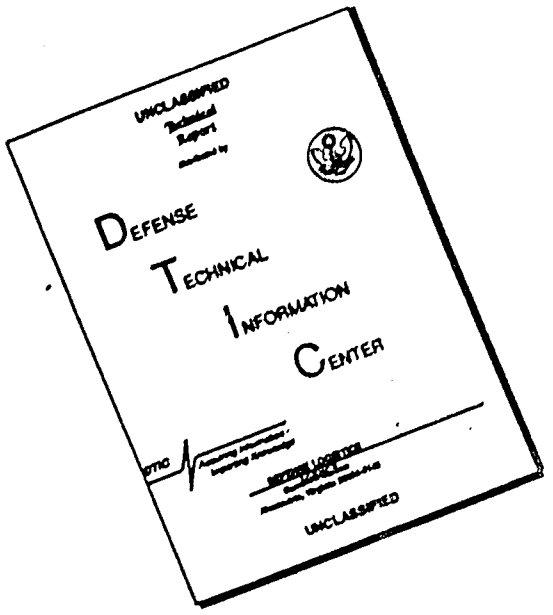

THIS DOCUMENT IS BEST QUALITY AVAILABLE. THE COPY FURNISHED TO DTIC CONTAINED A SIGNIFICANT NUMBER OF PAGES WHICH DO NOT REPRODUCE LEGIBLY.

BSD-TR-65-303 RESEARCH REPORT 226

MEASUREMENTS OF THE RADIATION FROM AN ABLATION CONTAMINATED BOUNDARY LAYER UNDER SIMULATED FLIGHT CONDITIONS

by

K. L. Wray, P. H. Rose and H. E. Koritz

AVCO-EVERETT RESEARCH LABORATORY
a division of
AVCO CORPORATION
Everett, Massachusetts

August 1965

supported jointly by

BALLISTIC SYSTEMS DIVISION
DEPUTY FOR BALLISTIC MISSILE RE-ENTRY SYSTEMS
AIR FORCE SYSTEMS COMMAND
Norton Air Force Base, California

under Contract No. AF 04(694)-414

ADVANCED RESEARCH PROJECTS AGENCY
monitored by the
ARMY MISSILE COMMAND
UNITED STATES ARMY
Redstone Arsenal, Alabama

under Contract No. DA-19-020-AMC-0210
(part of Project DEFENDER)

FOREWORD

This report has been supported by Avco-Everett Research Laboratory under Contract No. AF 04(694)-414 for Ballistic Systems Division, Deputy for Ballistic Missile Re-entry Systems, Air Force Systems Command, Norton Air Force Base, California. The secondary report number as assigned by AERL is Avco-Everett Research Laboratory Research Report 226. The Air Force program monitor for this contract is Thomas W. Swartz, 2nd Lt., USAF, Project Officer.

Publication of this report does not constitute Air Force approval of the report's findings or conclusions. It is published only for the exchange and stimulation of ideas.

Public release approval has been requested for this report for the purpose of submitting it for publication to the AIAA Journal.

Lieutenant Thomas W. Swartz, USAF
Project Officer

TABLE OF CONTENTS

ABSTRACT

This paper describes a 300 kW, 1 atmosphere arc jet facility which is capable of partially simulating the boundary layer produced on an ablating re-entry vehicle. The portion of the boundary layer from the ablating wall out to the maximum temperature is simulated. The simulation parameter developed is the ratio of the characteristic flow time in the boundary layer to the chemical time. Temperatures between 3000 and 6000°K are obtainable in the arc. In this range the arc-heated air is shown to be uniformly heated and in equilibrium. A method of positioning an ablative sample in the arc jet is described which produces a two-dimensional ablating boundary layer. An optical system is described which is capable of spatially resolving the boundary layer perpendicular to the ablating surface to better than 1/10 the boundary layer thickness. The integrated radiation emanating from this boundary layer has been studied with photomultipliers, and spatially resolved spectral plates have been taken. The air-Teflon boundary layer shows radiation from CF, Na and CN, while Delrin shows CN, Na, OH, NH, CH and H_α. Absolute boundary layer intensities have been measured on the air-Teflon system at 3869 ± 33 Å, which spans the CN (violet) (0, 0) sequence. By densitometering a spatially resolved spectral plate, the absolute intensity profile through an air-Teflon boundary layer has been evaluated for this radiation. At 5800°K this system is 20 times as intense as the free stream radiation in the same band pass, and at all temperatures studied it is the dominant boundary layer radiator in the visible, near IR and near UV. Experiments presently being carried out are described and future work is outlined.

1. Introduction

The ability to observe and investigate the pertinent reactions under simulated flight conditions in the laboratory would greatly enhance our understanding of the behavior of hot air-ablation product mixtures. The difficulty of laboratory duplication of Reynolds number and total enthalpy corresponding to the boundary layer of a re-entry vehicle is formidable. Requiring sufficient time to permit steady ablation further limits the choice of available experimental techniques.

In this paper we shall discuss the application of a technique first used by Rose and Offenhartz[1] to produce and measure turbulent boundary layer ablation rates. The method consisted of confining the flow issuing from a plasma generator to the inside of a pipe or channel. In such a flow the conditions inside the channel yield turbulent or laminar boundary layers which closely resemble those found on a re-entry vehicle.

The additional problem faced in this investigation was to attempt to simulate the chemical processes occurring in these boundary layers. In order to make this simulation general and also to circumvent the a priori lack of knowledge of the chemical processes involved in the gas mixtures, we have relied on a simple kinetic theory model to provide this simulation. We have simply asked that the collision rate between air and ablation species, at the energy level duplicating the boundary layer, be reproduced in the experiment representative of the desired flight conditions.

We have designed an experimental facility in which a two-dimensional boundary layer determined by these considerations can be observed with a spatial resolution of one-tenth the boundary layer thickness.

In the sections which follow, we shall present the details of this simulation principle and how it can be achieved in the laboratory, and describe the experimental facility which has been developed for this purpose and the diagnostic techniques used to date. Then we will discuss the preliminary results which have been obtained in this facility and their significance. Finally, experiments in progress and plans to further exploit this facility and gain a better understanding of the chemistry of the ablation process will be outlined.

2. Simulation Requirements

Since little is known about the ablated particles or their chemistry, it is not feasible to base the simulation requirements on chemical reaction times as would be desirable. Rather we turn to kinetic theory and examine the collision rate, for collisions of a given energy, E^*, of an ablated molecule in the boundary layer assuming constant collision cross sections. It is then possible to define a simulation parameter based on the number of such collisions an ablated molecule makes during the time τ_f it spends in the boundary layer. If we let τ_c be the average time between collisions, this simulation parameter may be expressed as the ratio

$$\frac{\tau_f}{\tau_c} = \int_0^{\tau_f} \frac{1}{n_i} \left(\frac{dn_{ij}}{dt}\right) dt, \qquad (1)$$

where[7, 3]

$$\frac{dn_{ij}}{dt} = 2\, n_i n_j \Omega_{ij} \bar{c}_{ij} e^{-E^*/kT} \left(\frac{E^*}{kT} + 1 \right) \qquad (2)$$

is the rate of binary collisions between species i and j in which the translational energy is greater than E^*, n_i and n_j are the number densities of species i and j, Ω_{ij} is the kinetic cross section, $2\bar{c}_{ij}$ is twice the relative mean thermal speed for the collision and is equal to $\bar{c}_j [1 + m_j/m_i]^{1/2}$, and T is the temperature. Substituting Eq. (2) into Eq. (1) and noting that the flow velocities for the species i and j are equal, we obtain

$$\frac{\tau_f}{\tau_c} = \left\{ n_j \Omega_{ij} L \frac{\bar{c}_j \left[1 + \frac{m_j}{m_i} \right]^{1/2}}{u_j} e^{-E^*/kT} \left(\frac{E^*}{kT} + 1 \right) \right\}_{AV.}, \qquad (3)$$

where L is the length of the boundary layer. For mixtures of masses of the same order and of approximately equal kinetic cross sections, the kinematic viscosity is

$$\nu_j = \frac{a \bar{c}_j}{\Omega_{ij} [n_i + n_j]} . \qquad (4)$$

Equation (3) may be rewritten

$$\frac{\tau_f}{\tau_c} = \left\{ a \sqrt{2}\, C_j \frac{Re_j}{M_j^2} e^{-E^*/kT} \left(\frac{E^*}{kT} + 1 \right) \right\}_{AV.}, \qquad (5)$$

where $Re_j = u_j L/\nu_j$ is the Reynolds number, $M_j = u_j/\sqrt{c}_j$ is the Mach number and $C_j = n_j/(n_i + n_j)$ is the fractional concentration of species j. If species j is air molecules, C_j will in general be of order unity; if species j is ablated molecules, C_j will be small. Under the above assumptions Re_j and M_j are always calculated for air. From Chapman and Cowling,[3] $a \simeq 1/2$ so that $a\sqrt{2} \simeq 1$.

For $E^*/kT \gg 1$, as is usually the case in chemical reactions, Eq. (5) is a strong function of temperature and the value of (τ_f/τ_c) will be largely determined by the maximum temperature in the boundary layer. Thus, it will be reasonable in general to evaluate the parameters in Eq. (5) at this point. It will be seen that the simulation parameter given by Eq. (5) is a function of Reynolds number, temperature, Mach number and relative particle density, which seems quite reasonable. Although it is not possible to duplicate the flight value of all of these parameters simultaneously in the arc facility, the resulting combination can be duplicated and they may be individually duplicated.

The net result of these considerations is that the flight situation is quite closely simulated in the inner portion of the boundary layer, i.e. up to the maximum temperature. In this region the collision partners and their environment are duplicated. Outside the maximum temperature region in the boundary layer the static temperature in the flight case drops rapidly while the experimental boundary layer essentially ends. This lack of simulation must be overcome by theoretical considerations. In the experiment we are able to examine the inner portion of the ablating boundary

layer in great detail under simulated flight conditions, and we can hope to develop a theoretical model which will explain our observations. In such a case we would have substantial confidence in the predictions made by this model for the flight situation which includes not only the inner portion of the boundary layer in which experimental verification has been achieved, but also the outer portion where we are unable to reproduce the phenomena.

We have computed the values of the parameters defined in the previous section for typical re-entry bodies and arc devices. Cones of 10° and 15° half angle flying a typical re-entry path have been selected for the re-entry bodies while, for the arc device, a plasma generator with a maximum energy of 500 kW in the gas is used. The plasma generator discharges into a plenum chamber and thence into a channel or pipe.

The simulation parameter defined by Eq. (5) has been evaluated at the point in the boundary layer where T is a maximum. The pipe of the arc device will have a subsonic or moderately supersonic boundary layer with a cold wall and T will be a maximum at the edge of the boundary layer. For the re-entry cone, a high Mach number boundary layer will exist and T will be a maximum at some point within the boundary layer.

We cannot estimate the activation energy E^* since we have no knowledge of the reaction path, and consequently we must duplicate the reaction partners and the maximum hypersonic boundary layer temperature. The factor $e^{-E^*/kT}\,(E^*/kT + 1)$ will then be duplicated, since we postulate that the same reactions will take place in either the hypersonic boundary layer or in the arc boundary layer.

Having duplicated the temperature maximum in the boundary layer, we need to evaluate the variations of the Mach number, Reynolds number and species concentration of the ablating species. At the present time we shall consider only laminar boundary layers, although by operating at higher pressures turbulent boundary layers can also be investigated.

In general, the fractional concentration of a given species through the boundary layer cannot be found without a detailed solution of the boundary layer equations. Thus, the value of C_j must be approximated. The ratio of the total mass of ablated material injected into the boundary layer per unit time and the total mass of air entering the boundary layer per unit time yields an approximation to this value.

The effective heat of ablation for an ablating material is defined as

$$H_{eff} = q_o/\dot{m}, \tag{6}$$

where q_o = heat transfer rate without ablation and $\dot{m}$ = mass rate of ablation. Assuming that the diffusion boundary layer is identical with the velocity boundary layer and that the ablative material sublimes, we can estimate the total ablation occurring over a distance x measured from the leading edge of the boundary layer. The total mass injected per unit time into the length of boundary layer is given by

$$\int_o^x \dot{m}dx = \int_o^x \frac{q_o}{H_{eff}}\, dx \simeq \frac{2q_o x}{H_{eff}}\,, \tag{7}$$

since $q_o \sim 1/\sqrt{x}$. The mass rate at which air flows into the same boundary layer is

$$\int_o^{\delta(x)} \rho\, U\, d\, y \simeq \rho_e\, U_e\, \delta\,(x), \tag{8}$$

where subscript e designates conditions external to the boundary layer. Defining the ratio of these quantities as the mass fraction of ablated material, C_j', it follows that

$$C_j' \simeq \frac{1}{1 + \dfrac{\rho_e U_e\, (\delta/\sqrt{x}) H_{eff}}{2\, q_o \sqrt{x}}} \tag{9}$$

Note that this procedure yields C_j' independent of x, since to a first approximation $\delta \sim \sqrt{x}$. As long as the molecular weights of the ablated products and air species are not too dissimilar, the fractional concentration, C_j, will be approximately equal to the mass fraction C_j'. For Teflon with its C, F, CO, CN, CF_2, etc., this is a reasonable approximation which, however, could be improved by additional calculations.

The classical incompressible laminar boundary layer thickness is given by[4]

$$\delta = 5 \left(\frac{\mu_e x}{\rho_e U_e} \right)^{1/2} \tag{10}$$

for the flat plate. In the case of a cone, the numerical constant in Eq. (10) must be divided by $\sqrt{3}$ and x should be interpreted as the distance from the apex of the cone. For the cases considered here, boundary layer thicknesses calculated from the dissociated gas, variable $\rho\mu$ theory of

Fay and Riddell[5] differed by only 10% from the values calculated from Eq. (10).

The ratio of the boundary layer thickness for an ablating surface to the nonablating value above may be written approximately as the ratio of the two heat transfer rates,[1] thus

$$\frac{\delta_{abl}}{\delta} = \frac{q_o}{q_{abl}} = \frac{H_{eff}}{C_{p_w} T_w + h_v} , \qquad (11)$$

where h_v is the heat of vaporization of the ablating material and the subscript w refers to wall conditions.

For cones, the heat transfer rate for the nonablating case, q_o, can be obtained from an extension of the work of Kemp, Rose and Detra.[6] For small cone angles, where the velocity on the cone, U_e, is approximately equal to the free stream velocity, their results can be written as

$$\frac{q_o}{q_{os}\sqrt{R_s}} = \left(\frac{3}{4\sqrt{2}}\right)^{1/2} \left(\frac{P_e U_e (\rho_s)^{1/2}}{P_s^{3/2} x}\right)^{1/2} ,$$

where R is the radius of the stagnation point, defined by subscript s.

Using the stagnation point heat transfer rate, $q_{os}\sqrt{R_s}$, as given approximately by Detra, Kemp and Riddell,[7] we can write an equation for the heat transfer parameter, $q_o\sqrt{x}$, needed in Eq. (9):

$$q_o\sqrt{x} \simeq 632 \left(\frac{P_e U_e (\rho_s)^{1/2} \rho_e}{P_s^{3/2} \rho_{SL}}\right)^{1/2} \left(\frac{U_e}{10^4}\right)^{3.15} . \qquad (12)$$

In Eq. (5) the Reynolds and Mach numbers are to be evaluated at the maximum temperature point in the boundary layer. The temperature of a cone boundary layer reaches a maximum at a point within the boundary layer at hypersonic Mach numbers. To determine this temperature we use the Crocco integral to determine the static enthalpy maximum, h_{max}, and assume T_{max} to occur at this point. Thus

$$h = h_w + (h_{es} - h_w) \frac{U}{U_e} - \frac{1}{2} U_e^2 \left(\frac{U}{U_e}\right)^2 ,$$

from which

$$U_{h\ max} = \frac{h_{es} - h_w}{U_e} ,$$

and

$$h_{max} = h_w + \frac{1}{2} \left(\frac{h_{es} - h_w}{U_e}\right)^2 . \qquad (13)$$

The density at the maximum temperature follows, since the pressure in the boundary layer is constant at the external value, P_e.

For the arc the conditions can be calculated more easily. If the channel wall boundary layer is thin with respect to the diameter of the channel, then

$$E_{eff} = \rho_e U_e A h_s ,$$

where E_{eff} = energy imparted to the gas by the arc (500 kW), h_s = stagnation enthalpy of the gas, and A = channel area. This determines the size of the arc device.

For the channel boundary layer the maximum temperature conditions are the conditions in the channel external to the boundary layer. The

parameters leading to the evaluation of (τ_f/τ_c) for the arc device have been calculated for several values of h_s and P_s, i.e., $(h_s/R_1 T_1) = 50$, 100, 200, 300, and $0.1 < P_s < 10$ atm. Equilibrium air charts[8] were used to determine T_s, ρ_s, and sound speed a_o. The local value of the viscosity μ is determined from tabulations of the transport properties of equilibrium air.

The plenum gas is isentropically expanded to a preselected channel Mach number, utilizing the value of $\gamma = C_p/C_v = 1.2$ which was shown by Logan and Treanor[9] to be a reasonable average for the range of conditions selected here.

To determine $q_o \sqrt{x}$ in Eq. (9) the heat transfer parameter, $Nu_w/\sqrt{Re_w}$, has been used. For the laminar dissociated boundary layer on a flat plate, without dissipation, the relationship derived by Kemp, Rose and Detra[6] has been used to obtain

$$q_o \sqrt{x} = \frac{0.648}{\sqrt{2}} \quad \frac{\mu_w}{0.71} \quad \frac{\rho_w}{\rho_e} \quad \left(\frac{\rho_e \mu_e}{\rho_w \mu_w}\right)^{0.438} \left(\frac{\rho_e U_e}{\mu_w}\right)^{0.5} (h_e - h_w). \qquad (14)$$

The simulation parameter defined by Eq. (5) can now be calculated for the conical re-entry vehicles from Eqs. (9) through (13) and the arc experiment from Eqs. (9), (10), (11) and (14) along with equilibrium air charts. Figure 1 shows the results calculated in this manner for a P_s of two atomspheres, as a function of T_{max}, the maximum boundary layer temperature, i.e., the temperature which must be duplicated in the proposed simulation. It can be concluded that most of the range of values of (τ_f/τ_c)

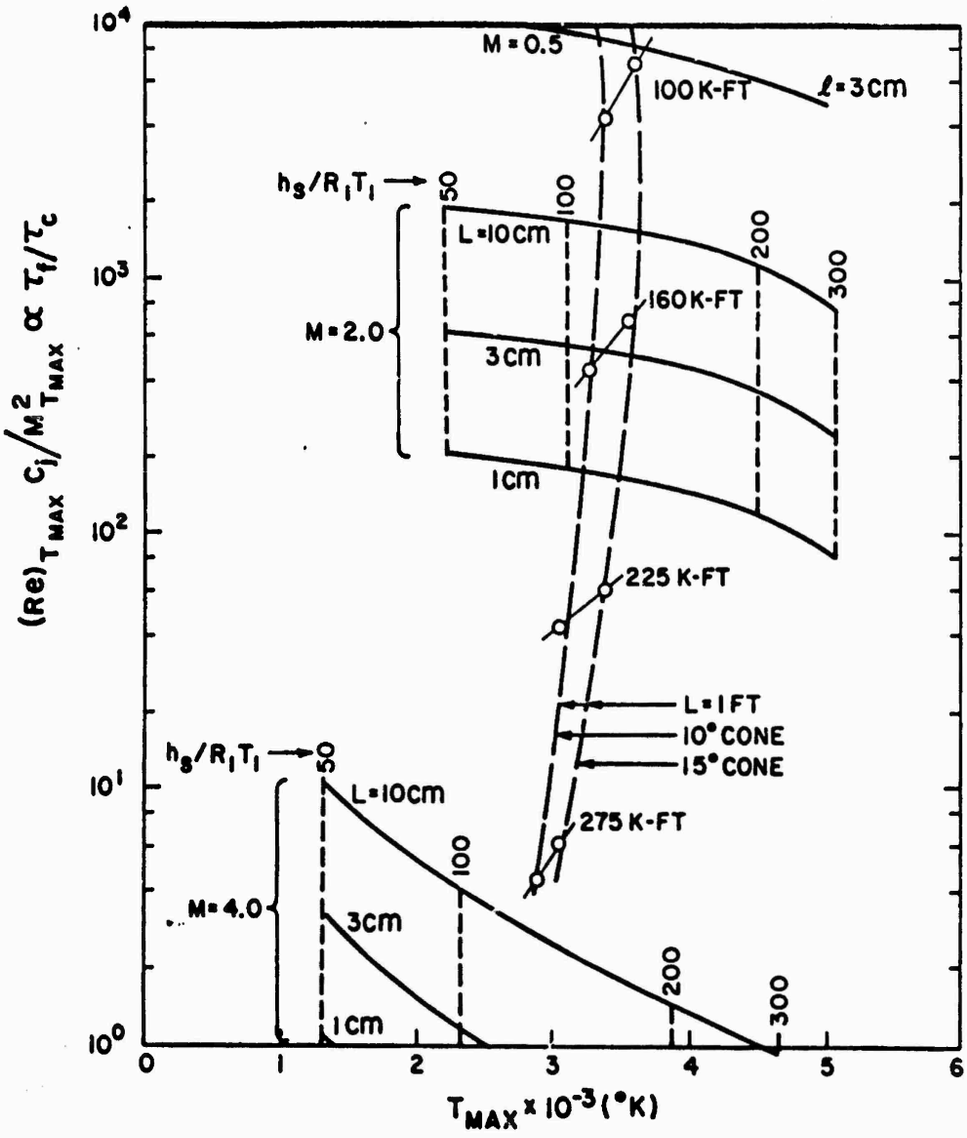

Fig. 1 Values of the simulation parameter, i.e., the ratio of the flow time to the chemical time as calculated for various operating conditions of the arc as well as those for conical re-entry bodies re-entering at 23,000 feet per second. This figure is based on a stagnation pressure of 2 atm.

A3641

needed to simulate the re-entry of conical bodies may be duplicated in an arc operating at a stagnation pressure of two atmospheres while simultaneously duplicating the maximum temperature. The choice of two atmospheres stagnation pressure was made to simplify the initial operation at $M \sim 0.5$ by allowing the air to exhaust into the ambient atmosphere. The calculations shown assume Teflon as the ablating material.

Not all of the individual parameters which when combined form τ_f/τ_c may be simultaneously duplicated in the arc. Duplication of the simulation parameter is primarily obtained by adjusting the Reynolds and Mach numbers to yield the correct value of the over-all parameter. The cone boundary layer Reynolds number may be duplicated in the arc boundary layer at any of the channel Mach numbers considered. Obviously the length of the channel is a free parameter with which some variation of Reynolds number can be achieved. The Mach number at the maximum temperature point in the boundary layer, however, can only be duplicated by operating the arc at Mach > 2. It is not possible to duplicate the value of C_j precisely over any range; however, the value of C_j for the arc channel boundary layer is never more than a factor of 3 different from that for the cone boundary layer.

We have shown that the chemistry of the ablation contaminated hypersonic boundary layer of a conical vehicle may be simulted in an arc plasma generator assuming, of course, that the simulation parameter suggested has the postulated significance. The calculations which have been made are quite approximate and should be relied on only for trends. However, we have attempted to show that we can operate in the proper range of the critical parameters. For further and more quantitative use

of the results to be presented here we can and must rely on a theoretical model to bridge the gap between the experiments and full scale flight.

3. Arc Facility

The design of the arc facility used in the present experiments was based on an arc developed at the Research and Advanced Development Division of Avco.[10] Figure 2 is a schematic drawing of the arc used for the present investigation. Nitrogen is introduced into (A) in a flow direction tangential to the tungsten tipped cathode. This results in a spiraling flow around the cathode as the gas moves into (B). The vortex flow stabilizes the arc by constricting the arc to the anode center. The oxygen is introduced downstream by means of twelve radial holes circumferentially placed at the entrance to the plenum chamber (C). Uniform mixing is assumed to occur within the plenum chamber and the hot air exits through the calorimeter section (D). All internal components of the arc are constructed of copper (except the cathode tip).

The exit nozzle consisting of the calorimeter section holder (F) and calorimeter section (D) had either a circular cross-section 3/4" in diameter or a rectangular cross-section 1/2" high by 1" wide. For the purpose of gross measurements of the ablation boundary layer radiation, the cylindrical calorimeter section is replaced by a pipe made of the ablating material. When it is desired to spatially resolve the boundary layer radiation, the ablating sample block is placed at the exit of the rectangular calorimeter section flush with the bottom surface. For the purpose of studying free stream radiation, either the circular or rectangular copper calorimeter sections may be used.

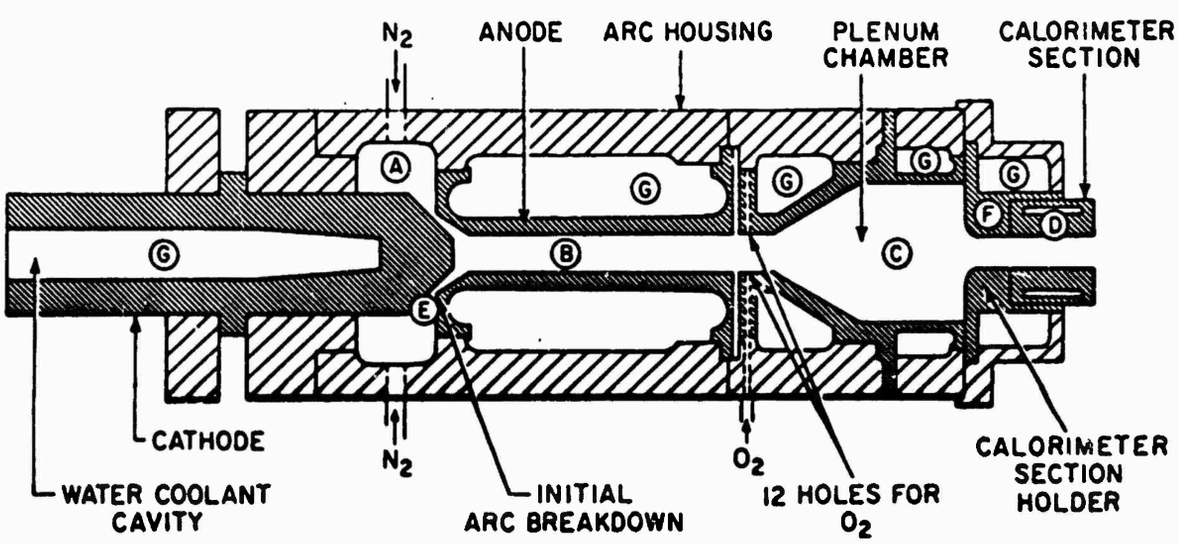

Fig. 2 Schematic diagram of arc used to obtain high temperature air. N_2 is introduced tangential to cathode at (A). O_2 is introduced downstream through twelve holes and mixing occurs in plenum chamber (C). Hot air exits through calorimeter section (D).

A3656

The arc is started by means of a capacitor discharge across the separation between cathode and anode at E and is "blown" downstream by the N_2 flow to a position to give stable arc operation. The total electrical power put into the arc is increased in steps by switching in individual (water cooled) 0.924 ohm resistors in parallel, thus reducing the ballast resistance which is in series with the battery bank power supply and the arc. The gas power is calculated by subtracting the wall losses from the arc power. These losses are obtained by measuring the temperature rise ΔT and the flow rate of the coolant water $\dot{m}$ (see (G), Fig. 2). The enthalpy per unit mass of gas H is then given by

$$H = \frac{VI - (S\,\dot{m}\,\Delta T)_{H_2O}}{\dot{m}_{AIR}} , \qquad (15)$$

where S is the specific heat of water and $\dot{m}_{AIR}$ is the sum of the mass flow rates of the O_2 and N_2.

Total arc power ranged from 80 kW to 330 kW. At a total arc power of 152 kW and an air mass flow rate of 46.2×10^{-3} lbs/sec an arc efficiency of 60.4% was observed. The equilibrium air temperature was 3070°K. At a total arc power of 330 kW and an air mass flow rate of 22.3×10^{-3} lbs/sec an arc efficiency of 38.3% was observed. The equilibrium air temperature was 5590°K.

Radiation data were obtained using an f/10 Hilger prism spectrograph (Kodak 103-F film) and a Bausch and Lomb grating monochromator along with an external optical system consisting of two 45° mirrors, a 24" focal length spherical mirror (located equidistant between arc light source and instrument slit), and an aperture which serves as a limiting stop for the

optical system. Figure 3 shows a schematic diagram of the optical system. The distance between the instrument slit and the arc light source is four times the mirror focal length so that the magnification is unity. The 1/4" diameter aperture limiting stop is placed in the external optical system at the mirror focal length. Hence, the solid angle subtended by the optical system is 8.5×10^{-5} steradians resulting in a resolution of 0.13 mm for a 1" optical path (i.e. for the rectangular nozzle). Diffraction limitation is negligible. The spectrograph has a magnification of 0.88 and a dispersion at $\lambda = 3900$ Å of 33 Å/mm for quartz optics and 11 Å/mm for glass optics. The monochromator has a dispersion of 33 Å/mm independent of wave length.

Figure 3 also shows a sketch of how the ablation sample is positioned with respect to the end of the arc apparatus. Also shown is the location of the slit image during a typical ablation run. It takes about 7 seconds for the thermistors monitoring the coolant water temperature to reach steady state. If the ablation sample was exposed to the arc gases from the time the arc was struck until the desired operating conditions were obtained, it would be severely ablated and a valley would be produced hiding the boundary layer. To alleviate this difficulty a solenoid unit was built which moved the ablating sample up to the bottom of the rectangular calorimeter section subsequent to steady state operation of the arc.

4. Experimental Results

4.1 Clean Air

As described in the previous section, the temperature is determined from energy balance considerations in the arc. In order to check these temperatures and to determine the temperature range under which the

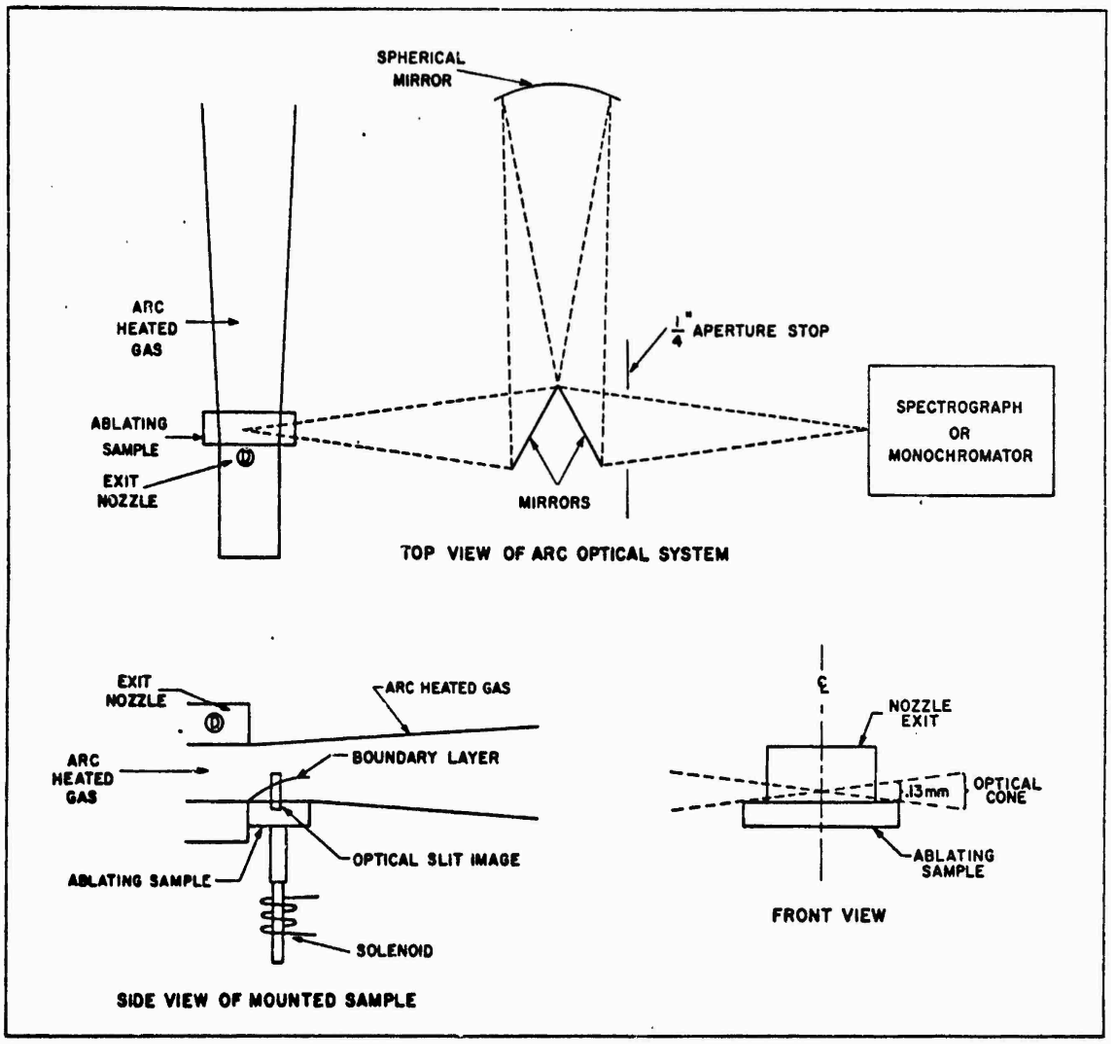

Fig. 3 Schematic diagram of optical system. Also shown is the method of mounting the ablating sample to obtain spatially resolved boundary layer radiation information.

A3629

arc heated air can be considered to be uniform throughout the gas exiting from the nozzle; a number of experiments were performed on the uncontaminated gas. These experiments included taking spectra to identify the radiating species[11] and their uniformity throughout the gas jet. Furthermore, quantitative spectral intensity measurements were made in a fixed band pass and these were compared to theory.

The clean air spectra showed the following molecular radiating systems: N_2^+(1-), N_2(2+), N_2(1+), O_2(Schumann-Runge), NO(γ) (requires longer exposure), and various atomic lines of nitrogen and oxygen. The three nitrogen systems tend to dominate the free-stream spectra at high temperatures whereas the O_2(S-R) and NO(β) tend to dominate at lower temperatures. It should be pointed out that the NO(β) system has not been identified in the air spectra, however, its presence is surmised from the data as will be described shortly. This lack of identification is in keeping with our knowledge of the NO(β) system[12] which, when in thermal equilibrium, exhibits very little structure, appearing almost as a broad continuum. Examples of the free stream spectra are given in Figs. 5 (high temperature) and 6 (low temperature) below; the free stream systems are identified at the top of each spectra. Copper is always seen as an impurity in the free stream spectra. Absolute intensity measurements of the 4022.7 Å Cu line indicate copper concentrations of the order of 10 parts/million.

Measurements of the absolute intensity averaged over the boundary layer were made using a calibrated photomultiplier (DuMont 6291) and the monochromator and external optical system described in Section 3. The band pass chosen to make these measurements was 3869 $\pm$ 33 Å, since

this encompasses the (0, 0) sequence of the CN (violet) system, a dominant radiator in the ablating boundary layer to be discussed below. The same band pass was used for measurements in the free stream. In reducing the data the optical path length was taken to be 1" in the case of the rectangular nozzle and 3/4" in the case of the circular nozzle. The free stream air data are shown in Fig. 4 where the intensity in watts/cc-ster is plotted against the temperature (obtained from arc energy balance). The data shown cover a temperature range of 3200-5900°K.

The solid lines shown in Fig. 4 are theoretically computed using electron transition moments and radiation equations given in the review paper of Keck, Allen and Taylor.[13] These theoretical intensities are, of course, calculated for the band pass 3869 $\pm$ 33 Å. The dashed line gives the sum of these theoretical components to the radiation. It is seen that above about 3500°K the data agree well with the theoretical curve. Below 3500°K data progressively fall higher than the theoretical curve. Indeed, free stream data were taken at temperatures as low as 2500°K and continue to deviate in this manner. Free stream spectra taken at these lower temperatures clearly indicate that the arc no longer produces a uniformly heated gas jet, but shows a hot core which is responsible for the data deviating in this manner from the theoretical curve. Between 4500 and 5500°K the slight deviation of the data from the theoretical curve might be due to an uncertainty in the electronic transition moment for the NO(β) system.

It should be pointed out that the free stream spectra shown in Figs. 5 and 6 in the vicinity of 3869 Å bear out the dominance of the O_2(S-R) [and NO(β)] at low temperature and the onset of the N_2^+(1-) and N_2(2+) at high temperature.

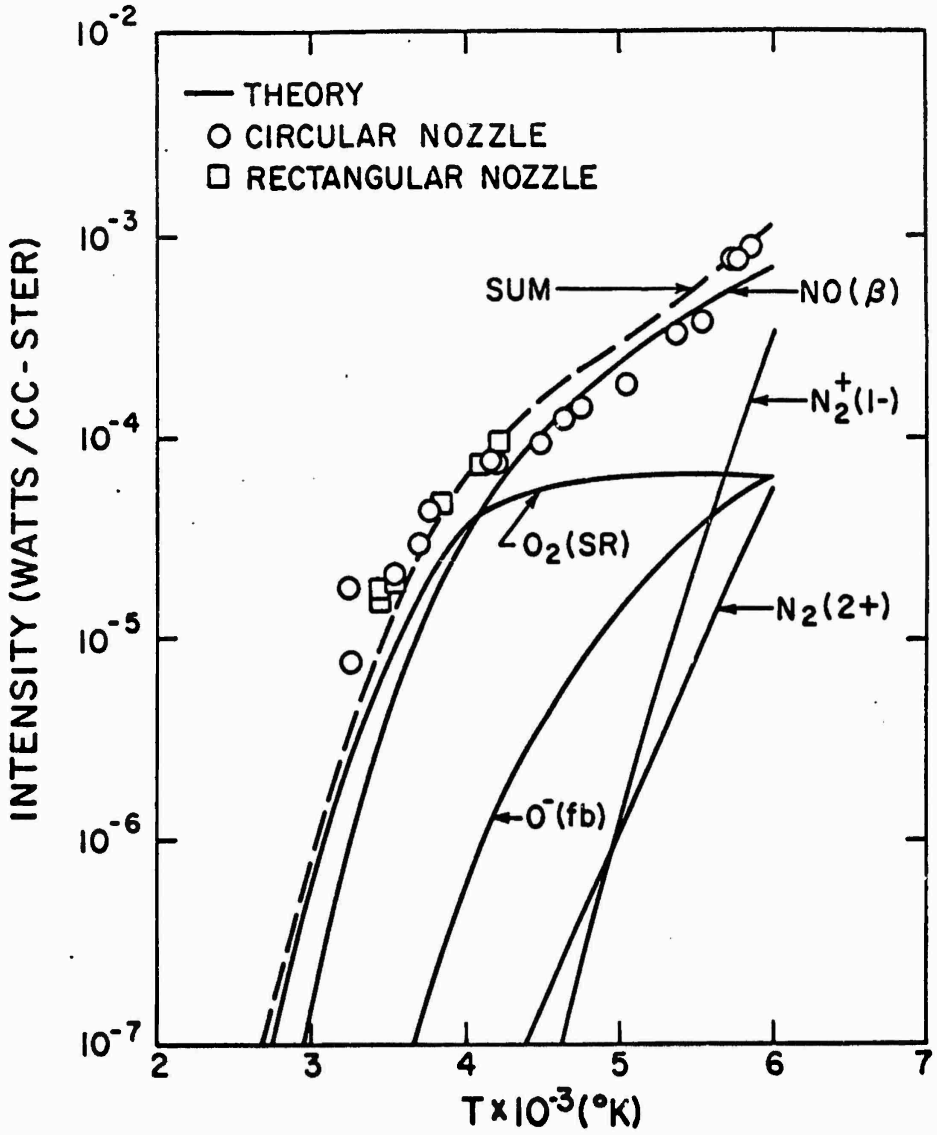

Fig. 4 Free stream air intensity vs. temperature at 3869 ± 33 Å. The experimental data is compared with the theoretical radiation.

A3687

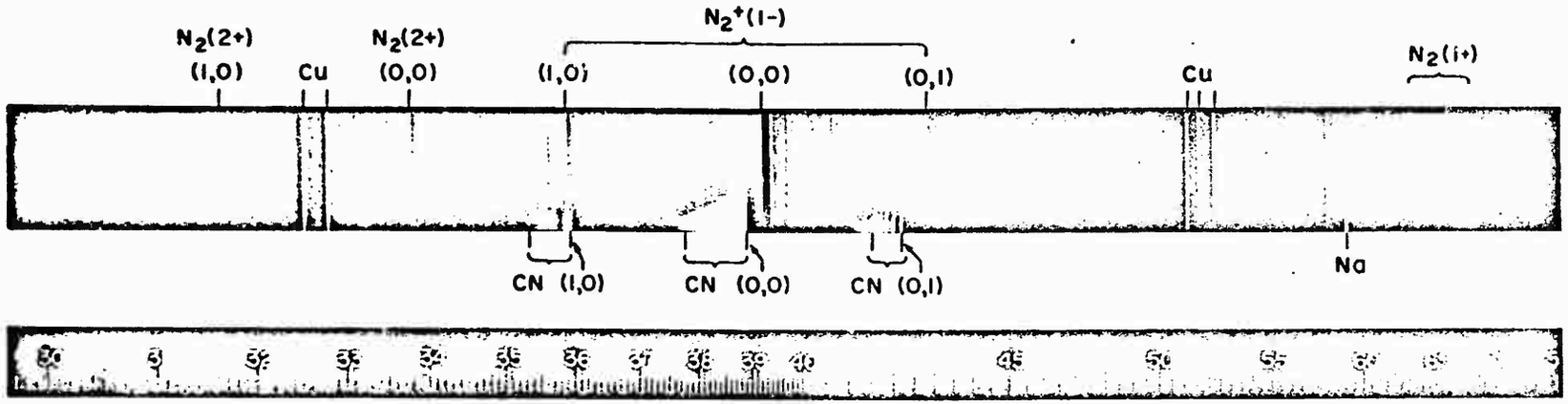

Fig. 5 Spatially resolved spectrum of boundary layer above Teflon ablating in arc heated air. The surface of the Teflon is at the bottom of the spectrum. Free stream temperature equals 5800°K, exposure 1 sec, limiting optical aperture is 1/4 inch diameter.

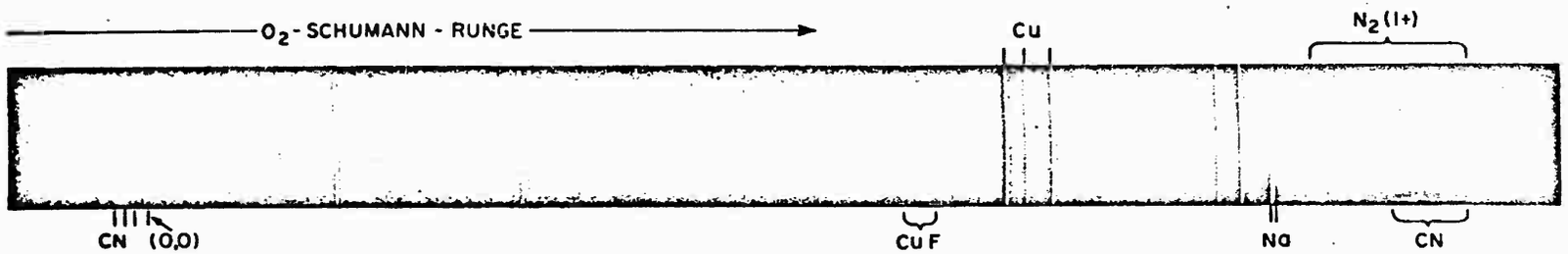

Fig. 6 Spatially resolved spectrum of boundary layer above Teflon ablating in arc heated air. The surface of the Teflon is at the bottom of the spectrum. Free stream temperature equals 3950°K, exposure 5 sec, limiting optical aperture is 3/4 inch. (Poor spatial resolution.)

Finally, it might be mentioned that some emissivity temperatures of the N_2^+ (1-) (0, 1) band head at 4278 Å were made which agreed well with the arc energy balance temperature. From the random fluctuations on the oscilloscope trace of such measurements, it was estimated that the temperature fluctuations (at about 6000°K) were of the order of several hundred degrees.

The above experiments demonstrate the satisfactory operation of the arc facility at temperatures above approximately 3500°K.

4.2 Ablating Boundary Layer

Figures 5 and 6, which have already been referred to with respect to the free stream portion of the spectrum, also show the spatially resolved air-Teflon boundary layer. The components radiating in the boundary layer are called out along the bottom of the spectra. It is seen that at both temperatures the sodium doublet at 5890 Å appears. It should be pointed out that the amount of sodium radiation varies considerably among different batches of Teflon. To date, no quantitative measurements have been made on the sodium radiation and no attempt has been made to control the sodium impurity present in the ablating sample.

The high temperature (free stream T = 5800°K) spectrum shown in Fig. 5 shows the CN (violet) (0, 0) (λ = 3883 Å), (0, 1) and (1, 0) sequences in the boundary layer. About 90% of the intensity is in the (0, 0) sequence. Careful inspection will also show the beginning of the CN (red) system around 6500 Å in the boundary layer. This spectrum was taken with quartz optics. Figure 6 taken at a free stream temperature of 3950°K shows only the strongest CN (violet) sequence, i.e., (0, 0). The CN (red) system can

again be seen in the boundary layer. Furthermore, one sees the CuF system at 4932 Å ($c^1\pi \rightarrow x^1\Sigma$).[11] The CuF is only seen in the boundary layer when the free stream temperature is low. This is probably related to the fact that the dissociation energy of CuF is about 3.0 eV.[14] However, one would expect to see it in an equilibrium boundary layer close to the surface where the temperature should be low even when the free stream temperature is high. Its absence in this case probably must be attributed to a nonequilibrium situation. When an air-Teflon boundary layer spectrum is greatly overexposed with no attempt made at spatial resolution, the CF system ($A^2\Sigma \rightarrow x^2\pi$) becomes apparent. These spectra are similar to those obtained by Wentink[15] covering the spectral region from 2200 to 2900 Å. No quantitative measurements have been made of the CF system.

Figure 7 shows a spatially resolved air-Teflon boundary layer spectrum, greatly enlarged, just covering the (0, 0) through (4, 4) sequence of CN (violet). The arc energy balance temperature for this run was 5810°K. Also indicated in this figure is a distance scale normal to the Teflon surface. The broad white mark which serves to locate the zero on this distance scale is a helium line taken with a wide slit. The helium lamp was placed behind a razor blade stop set at the level of the Teflon surface and the spectrum was taken before the arc run was made.

This CN spectrum was taken specifically for the purpose of densitometry; calibration data were taken on the same plate. The spectrum shown was scanned with a densitometer parallel to the Teflon surface with a slit 0.1 mm high and 0.01 mm wide. Nine such densitometer scans were made, each time moving out 0.1 mm (i.e., one slit height) from the

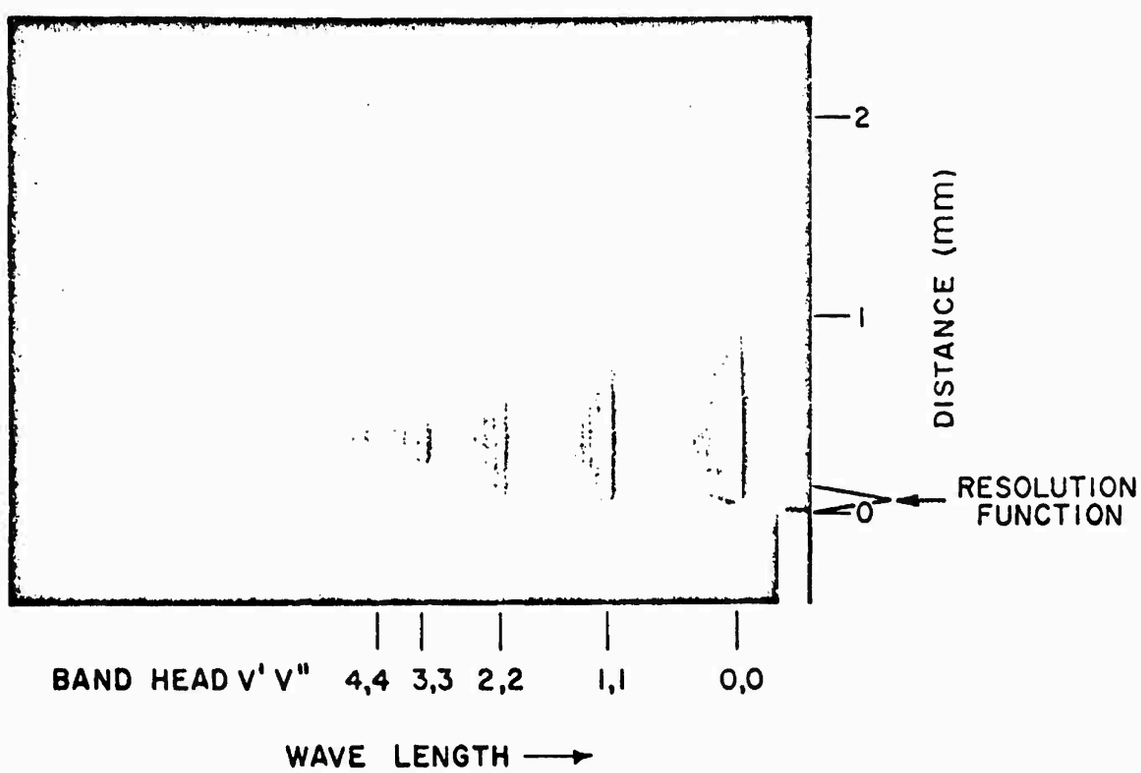

Fig. 7 Spatially resolved spectrum of boundary layer above Teflon ablating in arc heated air showing the CN (0, 0) through (4, 4) sequence enlarged. This plate was taken specially for densitometry. Free stream temperature equals 5810°K, exposure 1 sec, limiting optical aperture is 1/4 inch.

previous scan. These transmission vs. wave length densitometer curves were transformed into absolute intensity vs. wave length curves. The area under each of these nine curves was then obtained; thus the intensity in the CN (violet) (0, 0) sequence was evaluated as a function of distance through the boundary layer. These data are shown in Fig. 8. It should be pointed out that the intensity dip seen at 0.3 mm in the boundary layer can be identified in the spectrum (Fig. 7). It is clear that spectral data, like that shown in Fig. 7, can be used to deduce rotational and vibrational temperature profiles through the boundary layer. Preliminary work along these lines has begun.

By finding the area under the curve shown in Fig. 8 and dividing by the boundary layer thickness (1.6 mm), one obtains the average (0, 0) through (4, 4) CN radiation in the boundary layer which will be compared with integrated photomultiplier measurements discussed below.

Measurements of the average boundary layer radiation have been made using a calibrated photomultiplier. Once again the band pass investigated was 3869 ± 33 Å. In Fig. 9, we show a typical example of these data along with a photograph of the arc exit nozzle showing the Teflon sample raised to the position that it would be at during the run. Also shown is a photograph taken during the run with a filter over the camera lens which passes only 3869 ± 33 Å. The exposure for this photograph was 100 msec taken between 90 and 190 msec with the zero of time set when the solenoid pushing the Teflon sample was activated. The oscilloscope trace shown in this same figure shows the output of the photomultiplier which is monitoring the boundary layer radiation. The oscilloscope trace starts at zero time.

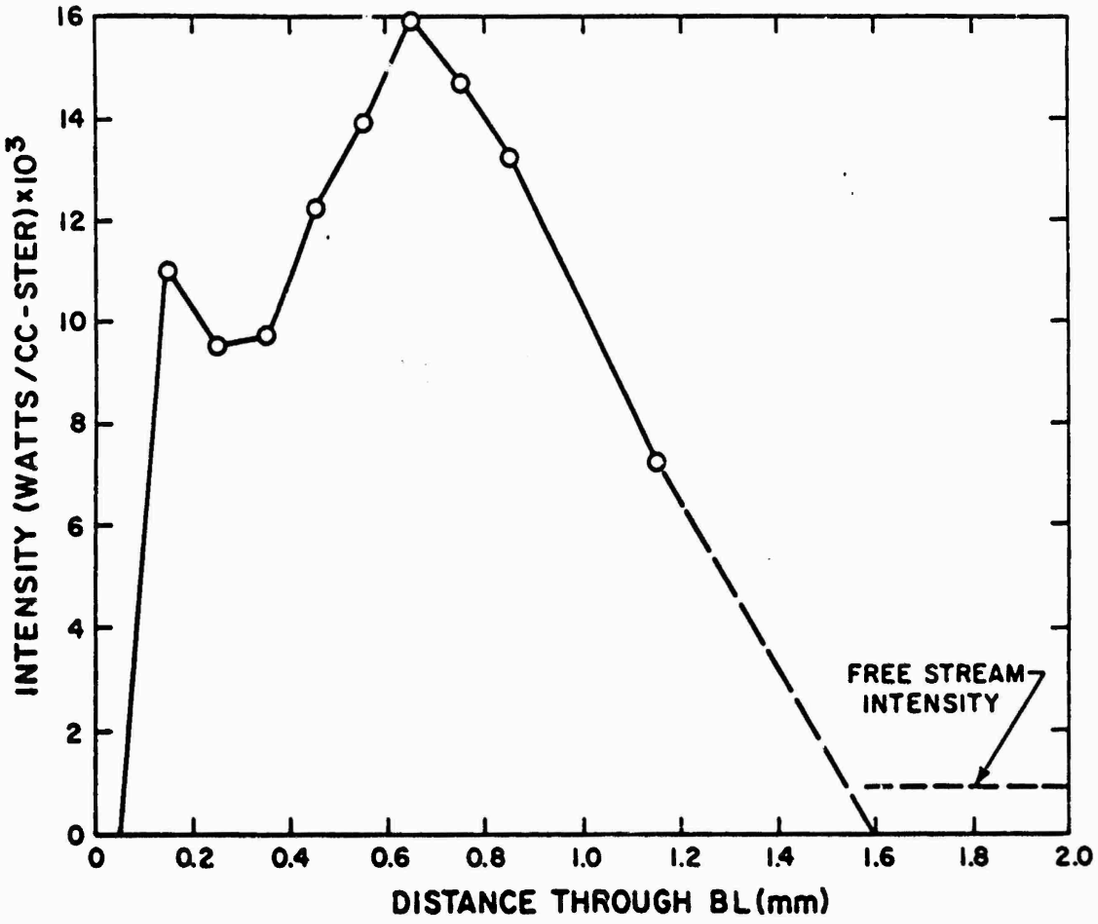

Fig. 8 The CN (0, 0) through (4, 4) intensity plotted against distance through the air-Teflon boundary layer. Free stream temperature equals 5810°K. The data are obtained from the spectrum shown in Fig. 7. The indicated free stream intensity is obtained from Fig. 4.

A2000

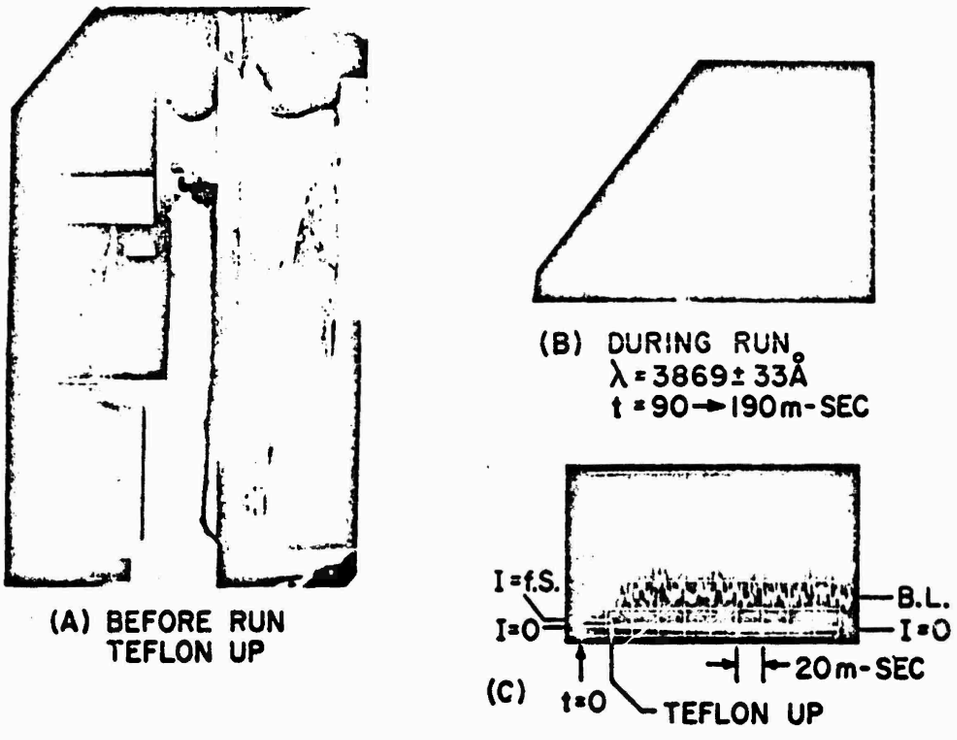

Fig. 9 Photograph of Teflon sample: A) Before arc is activated; B) During run; C) Shows output of photomultiplier monitoring boundary layer radiation at 3869 ± 33 Å. The free stream temperature in this run was 5180°K.

A3666

For the first 20 msec, the time it takes for the Teflon to be raised into position by the solenoid, a small signal is seen which corresponds to the free stream radiation. It then takes approximately 20 msec longer for a steady state boundary layer to form above the Teflon surface. Subsequent to that the radiation emanating from the boundary layer remains essentially constant.

This signal can be converted into the boundary layer radiation after correcting for the fact that only a portion of the slit is illuminated by the boundary layer radiation. The correction is accomplished via the equation

$$I_{B.L.} = I_t \frac{\ell_A + \ell_B + \ell_c}{\ell_B} - I_{f.s.} \frac{\ell_c}{\ell_B} \quad , \qquad (16)$$

where I_t is the total intensity indicated by the photomultipler output, $I_{f.s.}$ is the free stream radiation given by Fig. 4 and ℓ_A, ℓ_B and ℓ_c are the lengths of the slit which are below the Teflon surface, filled by the boundary layer, and filled by the free stream, respectively. ℓ_B is obtained by measuring the boundary layer thickness at the position of the slit image from photographs such as shown in Fig. 9(B).

These data are plotted in Fig. 10. Also shown on this figure is the single intensity measurement made by the densitometer measurements described above. At the lower temperatures the free stream radiation correction becomes important. The data points are plotted using the experimental values for the free stream radiation shown in Fig. 4. If, on the other hand, the theoretical value of the free stream radiation is used, the lowest temperature data points shown in Fig. 10 would be raised to the position of the arrowheads as shown in the figure. All the runs plotted

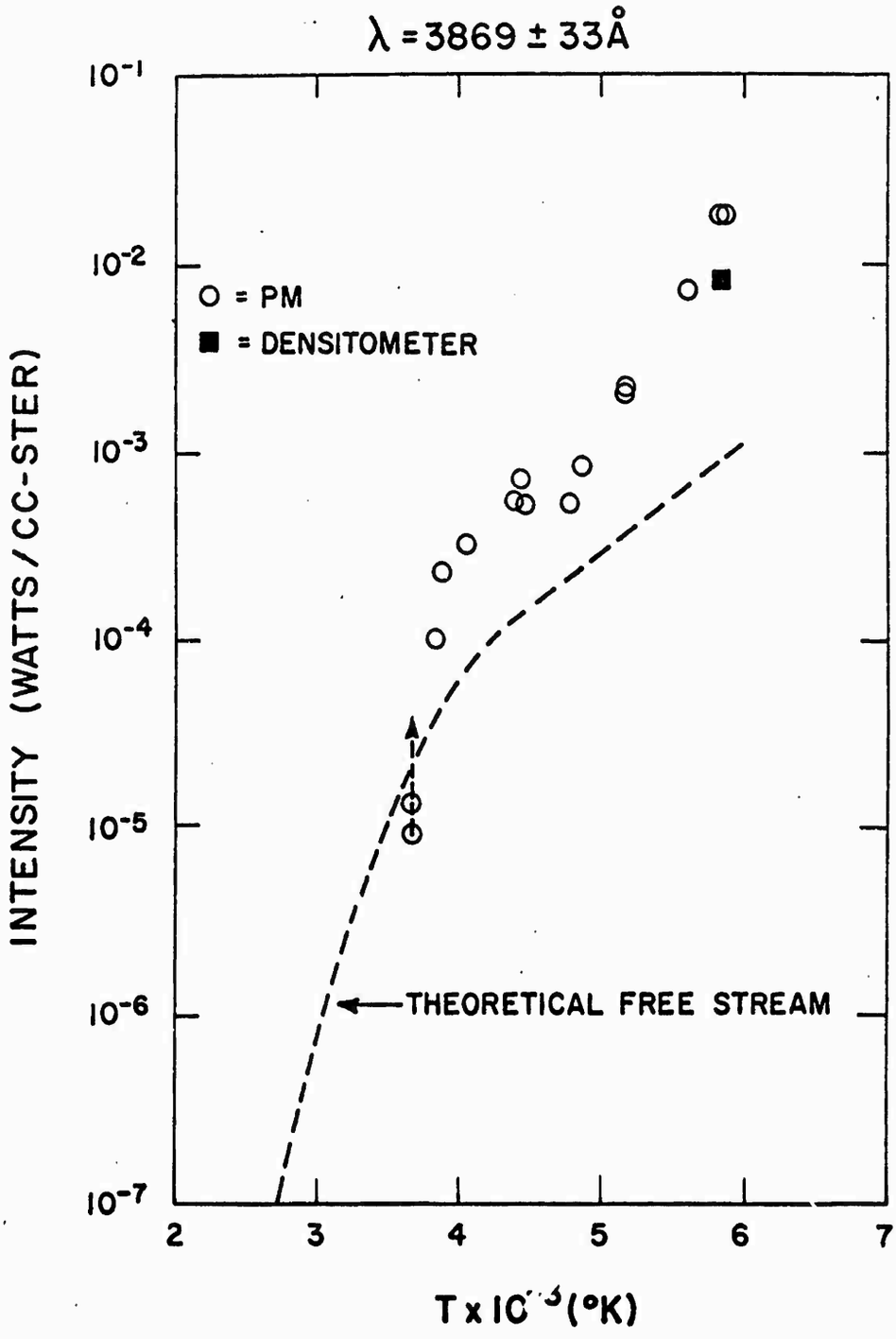

Fig. 10 Air-Teflon boundary layer intensity averaged through the boundary layer plotted against temperature. The experimental data are compared with the theoretical free stream intensity. The densitometer point was obtained by integrating the intensity curve shown in Fig. 8.

in Fig. 10 yielded boundary layer photographs similar to the one shown in Fig. 9(B) with the exception of the two lowest temperature runs (3675°K). These two runs showed no luminous boundary layers.

4.3 Delrin Air Boundary Layer

Although most of the boundary layer work described in this paper deals with the air-Teflon system, it should be pointed out that other materials have been examined in a qualitative manner. As an example we show in Fig. 11a spatially resolved air-Delrin spectrum. Delrin is a polyformaldehyde $(CH_2O)_n$. Free stream temperature equals 5880°K. Besides the CN (violet) and (red) systems and the sodium line that we have already described in the air-Teflon case, OH, NH and CH systems are also identified.[11] The H_α line is seen at 6563 Å. It is interesting to note that the CH system is seen only very deep in the boundary layer (the CH dissociation energy is 3.47 eV)[14] whereas the H_α line is seen only far out in the boundary layer (excited state at 12 eV).

5. Conclusions and Plans for Extension of Work

It is clear from the foregoing that the arc facility described in this paper is capable of producing a uniform equilibrium hot air jet at temperatures between approximately 3500 and 6000°K. A method of mounting a sample has been developed which produces a well defined two-dimensional ablating boundary layer which is simple enough in geometry so as to allow the gathering of data which can be treated and analysed by straightforward methods. As has already been mentioned in the previous section, work is now in progress to determine rotational and vibrational temperatures through the boundary layer. Also some preliminary measurements have been made using a liquid nitrogen cooled indium antiminide detector

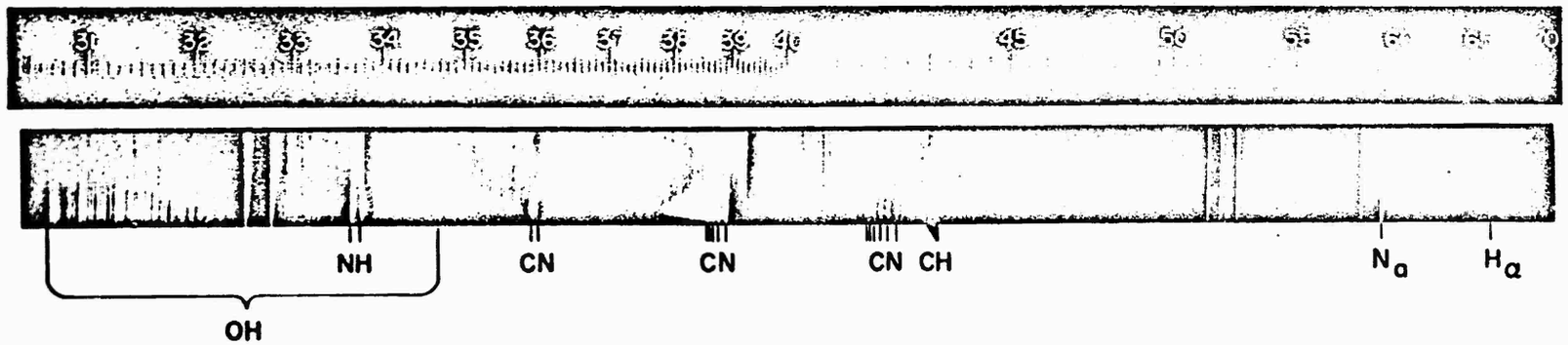

Fig. 11 Spatially resolved spectrum of boundary layer above Delrin ablating in arc heated air. The surface of the Delrin is at the bottom of the spectrum. Free stream temperature equals 5880°K, exposure 1 sec, stop is 1/4 inch.

(sensitivity to 5.7 μ). The CO vibrational-rotational system at 4.6 μ has been identified in the air-Teflon boundary layer. In order to get profiles of this CO radiation through the boundary layer, a horizontal scanning slit apparatus has been built which will allow the display of the indium antiminide signal on an oscilloscope as a function of distance through the boundary layer.

In the near future we plan to measure the ratio of the CN (red) to the CN (violet) intensities as a function of distance through the boundary layer, hence yielding an electronic temperature profile. Also contemplated is an experiment to measure the boundary layer conductivity employing the Q-coil technique.[16] This device has a response proportional to the conductivity times the radius to the fourth power. The Q-coil would be placed external to an ablating Teflon pipe, and hence the signal is most sensitive to the boundary layer conductivity.

The present optical system used in the emission studies could be readily adapted to doing absorption experiments simply by placing a light source on the opposite side of the arc from the present optical system. By doing absorption experiments we could identify and study molecules which exist only very near the ablating surface, and hence might be too cold to radiate.

Although it is not immediately contemplated, it seems quite feasible to use the line reversal technique (see, for example, Ref. 17) to measure the electronic temperature of some of the boundary layer species. And finally, it seems quite possible that the electron beam scattering technique developed by Camac for shock tube work[18] could be employed on the boundary layer arc experiment to determine density profiles through the boundary layer.

Up to the present time all the experimental work has been carried out at 1 atmosphere pressure. Recently the arc facility has been modified so as also to allow experiments to be done at reduced densities and supersonic flows as discussed in Section 2 of this paper.

Acknowledgments

We wish to acknowledge the early preliminary work done by Dr. Roy Heyman, while at this Laboratory, which was pertinent to the material covered in Section 2 of the paper. We thank Dr. Nelson Kemp for the benefit of many fruitful discussions, and finally we thank Mr. Leon Cohen for his aid in carrying out the experiment work.

REFERENCES

1. Rose, P.H. and Offenhartz, E., "Ablation Measurements in Turbulent Flow," Avco-Everett Research Laboratory Research Report 114 (August 1959). ARS Preprint 2009-61.

2. Fowler, R.H. and Guggenheim, E.A., Statistical Thermodynamics (Cambridge University Press, London, 1956) Chapter 12.

3. Chapman, S. and Cowling, T.G., The Mathematical Theory of Non-uniform Gases (Cambridge University Press, London, 2nd ed., 1952), Chapters 5 and 6.

4. Schlichting, H., Boundary Layer Theory (McGraw-Hill, New York, 1955).

5. Fay, J.A. and Riddell, F.R., "Theory of Stagnation Point Heat Transfer in Dissociated Air," J. Aero/Space Sci., 25, 73-85 (1958).

6. Kemp, N.H., Rose, P.H. and Detra, R.W., "Laminar Heat Transfer Around Blunt Bodies in Dissociated Air," J. Aero. Space Sci., 26, 421-430 (1959).

7. Detra, R.W., Kemp, N.H. and Riddell, F.R., "Addendum to Heat Transfer to Satellite Vehicles Re-entering the Earth's Atmosphere," Jet Propulsion, 27, 1256 (December 1957).

8. Feldman, S., "Hypersonic Gas Dynamics Charts for Equilibrium Air," Avco-Everett Research Laboratory Research Report 40 (1957).

9. Logan, J.G. and Treanor, C.E., "Tables of Thermodynamic Properties of Air from 3000°K," Cornell Aeronautical Laboratory Report BE-1007-A3 (1957).

10. John, R.R., Debolt, H., Hermann, M., Hogan, W., Kusko, A. and Liebermann, R., ASD-TDR 62-729, Part I. RAD-TR-63-3, 185, 204 (Run #31) (January 1963).

11. Pearse, R.W.B. and Gaydon, A.G., The Identification of Molecular Spectra (Chapman & Hall Ltd., London, 2nd ed., 1950).

12. Allen, R.A., "High Temperature Air Radiation Tables," to be published as Avco-Everett Research Laboratory Research Report.

13. Keck, J.C., Allen, R.A. and Taylor, R.L., "Electronic Transition Moments for Air Molecules," J. Quant. Spect. Rad. Transf., 3, 335-353 (1963).

14. Herzberg, G., Spectra of Diatomic Molecules (D. Van Nostrand Company, Inc., Canada, 2nd ed. 1951).

15. Wentink, T., Isaacson, L., Economou, G. L. and Flinn, D., "Ultraviolet Emission from CF Bands and Continua (Preliminary)," Avco RAD-TM-63-53 (July 31, 1963).

16. Koritz, H. E. and Keck, J. C., "A Technique for Measuring the Electrical Conductivity of Wakes of Projectiles at Hypersonic Speeds," Rev. Sci. Instr., 35, 201-208 (February 1964).

17. Gaydon, A. G. and Hurle, I. R., Eighth Symposium Combustion (Baltimore, Md., Williams and Wilkins, 1960) 309.

18. Camac, M., "Argon and Nitrogen Shock Thicknesses," Avco-Everett Research Laboratory Research Report 172 (December 1963); also AIAA Preprint 64-35.

Unclassified

Security Classification

DOCUMENT CONTROL DATA - R&D

(Security classification of title, body of abstract and indexing annotation must be entered when the overall report is classified)

1. ORIGINATING ACTIVITY (Corporate author)	2a. REPORT SECURITY CLASSIFICATION
Avco-Everett Research Laboratory 2385 Revere Beach Parkway Everett, Massachusetts	Unclassified
	2b GROUP

3. REPORT TITLE

MEASUREMENTS OF THE RADIATION FROM AN ABLATION CONTAMINATED BOUNDARY LAYER UNDER SIMULATED FLIGHT CONDITIONS

4. DESCRIPTIVE NOTES (Type of report and inclusive dates)

Research Report 226

5. AUTHOR(S) (Last name, first name, initial)

Wray, K. L., Rose, P. H., and Koritz, H. E.

6. REPORT DATE	7a. TOTAL NO. OF PAGES	7b. NO. OF REFS
August 1965	36	18

8a. CONTRACT OR GRANT NO.	9a. ORIGINATOR'S REPORT NUMBER(S)
AF 04(694)-414 b. PROJECT NO.	Research Report 226
c.	9b. OTHER REPORT NO(S) (Any other numbers that may be assigned this report)
d.	BSD-TR-65-303

10. AVAILABILITY/LIMITATION NOTICES

Qualified requesters may obtain copies of this report from DDC.

11. SUPPLEMENTARY NOTES	12. SPONSORING MILITARY ACTIVITY
	BSD - Deputy for Ballistic Missile Re-entry Systems AFSC, Norton AFB, California

13. ABSTRACT

This paper describes a 300 kW, 1 atmosphere arc jet facility which is capable of partially simulating the boundary layer produced on an ablating re-entry vehicle. The portion of the boundary layer from the ablating wall out to the maximum temperature is simulated. The simulation parameter developed is the ratio of the characteristic flow time in the boundary layer to the chemical time. Temperatures between 3000 and 6000 $^{\circ}$K are obtainable in the arc. In this range the arc-heated air is shown to be uniformly heated and in equilibrium. A method of positioning an ablative sample in the arc jet is described which produces a two-dimensional ablating boundary layer. An optical system is described which is capable of spatially resolving the boundary layer perpendicular to the ablating surface to better than 1/10 the boundary layer thickness. The integrated radiation emanating from this boundary layer has been studied with photomultipliers, and spatially resolved spectral plates have been taken. The air-Teflon boundary layer shows radiation from CF, Na and CN, while Delrin shows CN, Na, OH, NH, CH and H_α. Absolute boundary layer intensities have been measured on the air-Teflon system at 3869 $\pm$ 33 Å, which spans the CN (violet) (0,0) sequence. By densitometering a spatially resolved spectral plate, the absolute intensity profile through an air-Teflon boundary layer has been evaluated for this radiation. At 5800 $^{\circ}$K this system is 20 times as intense as the free stream radiation in the same band pass, and at all temperatures studied it is the dominant boundary layer radiator in the visible, near IR and near UV. Experiments presently being carried out are described and future work is outlined.

DD FORM 1 JAN 64 1473

Unclassified

Security Classification

14 KEY WORDS	LINK A		LINK B		LINK C	
	ROLE	WT	ROLE	WT	ROLE	WT
1. Radiation - Ablation effects						
2. Boundary layers - Radiation						
3. Re-entry vehicles, ablating - Radiation						
4. Ablation products						
5. Arc jets						
6. Teflon - Ablation						
7. Boundary layers - Simulation						
8. Delrin - Ablation						

INSTRUCTIONS

1. ORIGINATING ACTIVITY: Enter the name and address of the contractor, subcontractor, grantee, Department of Defense activity or other organization *(corporate author)* issuing the report.

2a. REPORT SECURITY CLASSIFICATION: Enter the overall security classification of the report. Indicate whether "Restricted Data" is included. Marking is to be in accordance with appropriate security regulations.

2b. GROUP: Automatic downgrading is specified in DoD Directive 5200.10 and Armed Forces Industrial Manual. Enter the group number. Also, when applicable, show that optional markings have been used for Group 3 and Group 4 as authorized.

3. REPORT TITLE: Enter the complete report title in all capital letters. Titles in all cases should be unclassified. If a meaningful title cannot be selected without classification, show title classification in all capitals in parenthesis immediately following the title.

4. DESCRIPTIVE NOTES: If appropriate, enter the type of report, e.g., interim, progress, summary, annual, or final. Give the inclusive dates when a specific reporting period is covered.

5. AUTHOR(S): Enter the name(s) of author(s) as shown on or in the report. Enter last name, first name, middle initial. If military, show rank and branch of service. The name of the principal author is an absolute minimum requirement.

6. REPORT DATE: Enter the date of the report as day, month, year, or month, year. If more than one date appears on the report, use date of publication.

7a. TOTAL NUMBER OF PAGES: The total page count should follow normal pagination procedures, i.e., enter the number of pages containing information.

7b. NUMBER OF REFERENCES: Enter the total number of references cited in the report.

8a. CONTRACT OR GRANT NUMBER: If appropriate, enter the applicable number of the contract or grant under which the report was written.

8b, &c, & 8d. PROJECT NUMBER: Enter the appropriate military department identification, such as project number, subproject number, system numbers, task number, etc.

9a. ORIGINATOR'S REPORT NUMBER(S): Enter the official report number by which the document will be identified and controlled by the originating activity. This number must be unique to this report.

9b. OTHER REPORT NUMBER(S): If the report has been assigned any other report numbers *(either by the originator or by the sponsor)*, also enter this number(s).

10. AVAILABILITY/LIMITATION NOTICES: Enter any limitations on further dissemination of the report, other than those imposed by security classification, using standard statements such as:

(1) "Qualified requesters may obtain copies of this report from DDC."

(2) "Foreign announcement and dissemination of this report by DDC is not authorized."

(3) "U. S. Government agencies may obtain copies of this report directly from DDC. Other qualified DDC users shall request through _____."

(4) "U. S. military agencies may obtain copies of this report directly from DDC. Other qualified users shall request through _____."

(5) "All distribution of this report is controlled. Qualified DDC users shall request through _____."

If the report has been furnished to the Office of Technical Services, Department of Commerce, for sale to the public, indicate this fact and enter the price, if known.

11. SUPPLEMENTARY NOTES: Use for additional explanatory notes.

12. SPONSORING MILITARY ACTIVITY: Enter the name of the departmental project office or laboratory sponsoring *(paying for)* the research and development. Include address.

13. ABSTRACT: Enter an abstract giving a brief and factual summary of the document indicative of the report, even though it may also appear elsewhere in the body of the technical report. If additional space is required, a continuation sheet shall be attached.

It is highly desirable that the abstract of classified reports be unclassified. Each paragraph of the abstract shall end with an indication of the military security classification of the information in the paragraph, represented as *(TS)*, *(S)*, *(C)*, or *(U)*.

There is no limitation on the length of the abstract. However, the suggested length is from 150 to 225 words.

14. KEY WORDS: Key words are technically meaningful terms or short phrases that characterize a report and may be used as index entries for cataloging the report. Key words must be selected so that no security classification is required. Identifiers, such as equipment model designation, trade name, military project code name, geographic location, may be used as key words but will be followed by an indication of technical context. The assignment of links, rules, and weights is optional.